Basement Membrane Structure In Situ: Evidence for Lateral Associations in the Type IV Collagen Network

Peter D. Yurchenco* and George C. Ruben‡

*Department of Pathology, University of Medicine and Dentistry of New Jersey–Robert Wood Johnson Medical School, Piscataway, New Jersey 08854; and ‡Department of Biological Sciences, Dartmouth College, Hanover, New Hampshire 03756

Abstract. To determine molecular architecture of the type IV collagen network in situ, the human amniotic basement membrane has been studied *en face* in stereo relief by high resolution unidirectional metal shadow casting aided by antibody decoration and morphometry. The appearance of the intact basement membrane is that of a thin sheet in which there are regions of branching strands. Salt extraction further exposes these strands to reveal an extensive irregular polygonal network that can be specifically decorated with gold-conjugated anti-type IV collagen antibody. At high magnification one sees that the network, which contains integral (9–11-nm net diameter) globular domains, is formed in great part by lateral association of monomolecular filaments to form branching strands of variable but narrow diameters. Branch points are variably spaced apart by an average of 45 nm with 4.4 globular domains per micron of strand length. Monomolecular filaments (1.7-nm net diameter) often appear to twist around each other along the strand axis; we propose that super helix formation is an inherent characteristic of lateral assembly. A previous study (Yurchenco, P. D., and H. Furthmayr. 1984. *Biochemistry.* 23:1839) presented evidence that purified murine type IV collagen dimers polymerize to form polygonal arrays of laterally as well as end-domain–associated molecules. The architecture of this polymer is similar to the network seen in the amnion, with lateral binding a major contributor to each. Thus, to a first approximation, isolated type IV collagen can reconstitute in vitro the polymeric molecular architecture it assumes in vivo.

THE structural scaffolding of basement membranes is formed by a polymerized network of type IV collagen (26, 29, 31) whose molecular architecture in situ has not been previously defined.

Our concepts about this polymeric structure have been derived principally from biochemical studies. The monomeric unit of the network is a 400–426-nm-long (26, 29) threadlike molecule with a globular domain at the COOH terminus (8). Proteolytic extraction studies (19, 26) on the Engelbreth-Holm-Swarm (EHS)[1] tumor matrix led to the identification of a binding site at each end of the monomer, each mediating the formation of a covalently stabilized complex: the amino termini of four monomers join together by a 30-nm end-overlap (1, 6, 17, 26) to form a four-armed tetramer (7S) and the COOH termini of two monomers join end-to-end to form a linear dimer (26). Timpl et al. (26) postulated that NH_2- and COOH-terminal binding accounts for the formation of an open polymeric network of type IV collagen. Yurchenco and Furthmayr (29), on the other hand, proposed that purified type IV collagen dimers self-assemble into a tighter polygonal network held together prominently by lateral (side-by-side) interactions as well as the end-domain interactions identified earlier. The in vitro self-assembled network had the appearance in rotary-shadowed replicas of an irregular polygonal array whose sides were from one to several triple helical strand thick and whose vertices were frequently occupied by the COOH-terminal globular domains. More recently evidence has been advanced (27) that the globular domain will itself bind type IV collagen along its chain and that this domain is important for lateral assembly.

Verification of polymer structure proposed from in vitro work has not been previously provided by structural analysis of basement membranes in tissue. In the electron microscope, basement membranes are seen to consist of a lamina densa bounded by one or two lamina rarae (7) with type IV collagen found in all layers (20). Some basement membranes have been described as having a fine meshwork of fibrils ~4 nm in diameter (7). Reichert's membrane has been reported to consist of parallel layers, each composed of 3–8-nm-thick cords, which, on plasmin digestion, become a meshwork of 1.5–2-nm filaments (12). Descemet's membrane, on the other hand, contains a regular collagenous hexagonal lattice within which can be found a finer irregular collagenous mesh (25). These and other studies, while providing important information on basement membrane morphology, have not revealed the molecular detail needed to validate competing structural models developed from in vitro data.

To study the molecular architecture of a type IV collagen

1. *Abbreviations used in this paper*: EHS, Englebreth-Holm-Swarm tumor; GuHCl, guanidine hydrochloride; NEM, *N*-ethylmaleimide.

network in situ, we have examined the basement membrane of the human amnion *en face* using a stereoscopic high resolution freeze-dry, unidirectional platinum replication technique for transmission electron microscopy (21–24), which has been used to visualize the molecular architecture of other biopolymers (21, 24). The amnion possesses a simple, continuous basement membrane that lies between a superficial cuboidal epithelial layer and a deeper collagenous stroma (13, 15, 16). This basement membrane can be exposed as a flat surface for replication analysis (13) and soluble components can be extracted, further exposing the collagen network. In this study we present evidence that this network, visualized in situ, is formed in significant part by lateral associations, and that supramolecular filament twisting is a characteristic of these associations.

Materials and Methods

Preparation of Amniotic Basement Membrane Surfaces

Normal term human placentas, obtained in a fresh state within 2 h after delivery, were rinsed in cold 10 mM sodium phosphate, pH 7.4, 127 mM NaCl (PBS). The amnion was blunt dissected from the chorionic plate. Sections of the amnion were mounted and oriented on plastic rings and stripped of the epithelial layer based upon the method of Liotta et al. (13). Briefly, the tissues were washed through several changes of cold 5 mM Tris-HCl, pH 7.4, with 0.5 mM diisopropylfluorophosphate, 1 mM EDTA, 1 mM *N*-ethylmaleimide (NEM) over a period of several hours and then incubated at 37°C in 4% sodium deoxycholate with 0.5 mM phenylmethylsulfonyl fluoride (PMSF), 2 mM EDTA, and 1 mM NEM for 90 min. The samples were transferred to PBS, wiped with wet gauze to remove the cell layer, washed with multiple changes of PBS in the cold, and mounted onto 1/2-inch diameter tissue holders. To deplete the exposed basement membranes of salt-dissociable macromolecules, preparations were incubated in the cold sequentially with: (*a*) 3.4 M NaCl in 50 mM Tris-HCl, pH 7.4, with 1 mM PMSF, 1 mM EDTA, 1 mM NEM for 1 h; (*b*) 1.7 M NaCl in the above buffer with inhibitors for 1 h; and (*c*) 4 M guanidine hydrochloride (GuHCl) in the above buffer with inhibitors for one to several hours. After washing with PBS, intact, salt-extracted, and antibody-decorated amnions were fixed in fresh 4% formaldehyde (prepared from paraformaldehyde) in PBS overnight in the cold, washed in PBS, and then transferred into 25 or 30% ethanol on ice.

Preparation and Evaluation of Type IV Collagen Antibody

Type IV collagen was extracted and purified from lathyritic murine EHS tumor as described (29). This protein, after dialysis into PBS at a concentration of 0.5–1 mg/ml, was mixed with complete Freund's adjuvant and used to immunize New Zealand white rabbits. Antiserum was collected and type IV collagen-specific antibody was purified by affinity chromatography using the collagen coupled in 0.2 M sodium bicarbonate to cyanogen bromide (CNBr)-activated Sepharose CL-4B (Pharmacia Fine Chemicals, Piscataway, NJ). Preimmune IgG (Miles Scientific, Napervile, IL) was cross-adsorbed on a type IV collagen affinity column. 96-well Linbro EIA microtitration plates (Flow Laboratories, McLean, VA) were coated with 0.1 ml per well of type IV collagen (0.1 mg/ml) in 40 mM sodium carbonate/bicarbonate buffer, pH 9.6. Subsequent incubation and wash steps were carried out in PBS containing 0.06% Triton X-100 and 0.1% BSA (RIA grade; Sigma Chemical Co., St. Louis, MO). After washing of the plates with the above buffer, wells were incubated with antibody in serial twofold dilutions or, for competition assays, at a concentration of 0.16 μg/ml in the presence of serial dilutions of competing protein. Each well was further washed and then incubated with 1:2000 horseradish peroxidase conjugated to protein A (Sigma Chemical Co.) and washed again. Color was developed by the addition of 150 μl/well of 0.1 mM *o*-phenylenediamine in 50 mM citric acid/100 mM sodium phosphate buffer containing 0.04% hydrogen peroxide for 5–10 min, followed by the addition of 50 μl of 2 M sulfuric acid. Spectrophotometric data was recorded with a Titertek Multiskan MC (Flow Laboratories) at 492 nm.

Purification of Macromolecules for Competition Binding Assays

Laminin and the 150,000-D form of nidogen were purified from lathyritic EHS tumor as described (18). The low density, high molecular mass form of basement membrane heparan sulfate proteoglycan was purified from lathyritic EHS tumor (30). This proteoglycan, similar if not identical to the low density form described by Hassel et al. (10), has a core protein of ~450,000 D and generally three heparan sulfate chains, each ~80,000 D. Briefly, tumor residue, after preextraction with 3.4 M and 1.7 M NaCl (29), was extracted with 5 M urea, 125 mM Tris-HCl, pH 7.4, with 0.5 mM DFP, 1 mM EDTA, 8 mM NEM. After centrifugation, the supernatant was bound onto DEAE-Sephacel (Sigma Chemical Co.) equilibrated in the same buffer containing 0.1% 3-[3-cholamidopropyl)-dimethylammonio]-1propane sulfonate and was eluted with a linear 0–0.8 M NaCl gradient. The large bound peak was mixed with solid CsCl to a density of 1.4 gm/cm^3 and centrifuged at 10°C for 68–72 h in a rotor (Ty65; Beckman Instruments, Inc., Palo Alto, CA). The central peak was pooled, dialyzed against 4 M GuHCl in Tris buffer, chromatographed on a Sephacryl S400 column, and stored in liquid nitrogen. Human types I, III, and V collagen were isolated from placenta and purified by salt fractionation in acetic acid and ion exchange chromatography (14). Type V collagen was compared by SDS-PAGE with a chick standard kindly provided by Dr. David Birk (Dept. of Pathology, UMDNJ-Robert Wood Johnson Medical School, Piscataway, NJ).

Direct Coupling of Antibody to 5 nm Colloidal Gold

Affinity-purified type IV antibody and preimmune IgG were coupled to 5 nm gold particles based upon a method recommended by Janssen Pharmaceuticals (Piscataway, NJ) and modified by Dr. David Birk (personal communication). Several milligram of antibody were dialyzed into 5 mM sodium phosphate buffer, pH 8.6, and then mixed with saturating amounts of 5-nm colloidal gold suspension (Janssen Pharmaceuticals). The mixture was then adjusted to 0.05% polyethylene glycol (MW 15-20 K), 0.01 M sodium phosphate, 0.27 M NaCl, pH 8.3, and 0.1% BSA, centrifuged for 20 min at 8,000 rpm in an SS34 rotor (Sorvall Instruments, Wilmington, DE), and the remaining suspended gold pelleted at 34,000 rpm in a Ty65 rotor for 45 min. The pellet was resuspended in several milliliters of PBS containing 0.1% BSA, 0.05% sodium azide and layered onto a 10–35% linear glycerol gradient in the above buffer. The samples were centrifuged in a rotor (SW40Ti; Beckman Instruments) in the cold at 30,000 rpm for 45 min. The dispersed antibody-bound gold was recovered from the middle third of the centrifuge tube, diluted in the above buffer, and adjusted to an A_{600} of 0.35.

Immunolocalization of Antibody by Light Microscopy

5-μm-thick frozen sections of human amnion and kidney (mouse and human) were prepared on albumin-coated glass slides. Sections to be treated with gold-treated antibodies were incubated in 4 M GuHCl buffer for 1 h on ice, washed with PBS, treated with freshly prepared 4% formaldehyde in PBS for one to several hours followed by incubation in 0.5 mg/ml of sodium borohydride in PBS. After washing in PBS, the sections were overlayed with 0.2 ml of antibody (5 μg/ml) or gold-coupled antibody (1/4 dilution) in PBS containing 0.1% BSA and 0.05% Tween 20 (Janssen Pharmaceuticals) for 1 h and then washed. Free antibody-treated specimens were overlayed with a 1:300 dilution of fluorescein conjugated sheep anti-rabbit IgG (Cooper Biomedical, Malvern PA), incubated at room temperature for 1 h, washed, mounted wet with a coverslip, and examined in a Zeiss microscope fitted for epifluorescence. Slides treated with gold-coupled antibodies were enhanced with a silver stain using a commercial kit (IntenSE; Janssen Pharmaceuticals), counterstained with hematoxylin, dehydrated, and mounted.

Decoration of Amniotic Basememt Membrane En Face with Gold-coupled Antibody for Platinum Replication

PBS-washed salt-extracted amniotic samples were prefixed in freshly prepared 4% formaldehyde in PBS on ice for 1 h, washed in PBS, and then treated with 0.5 mg/ml sodium borohydride in PBS in the cold for 1 h. After further washing with PBS the specimens were overlayed with a 1/4 dilution of either gold-tagged type IV collagen antibody or gold-tagged preimmune IgG in PBS, 0.1% BSA, 0.05% sodium azide, 0.05% Tween 20. The specimens were incubated at room temperature with constant rocking for 2 h. The amniotic samples were then washed with PBS over 90 min with multiple buffer changes, fixed on ice with fresh 4% formaldehyde overnight,

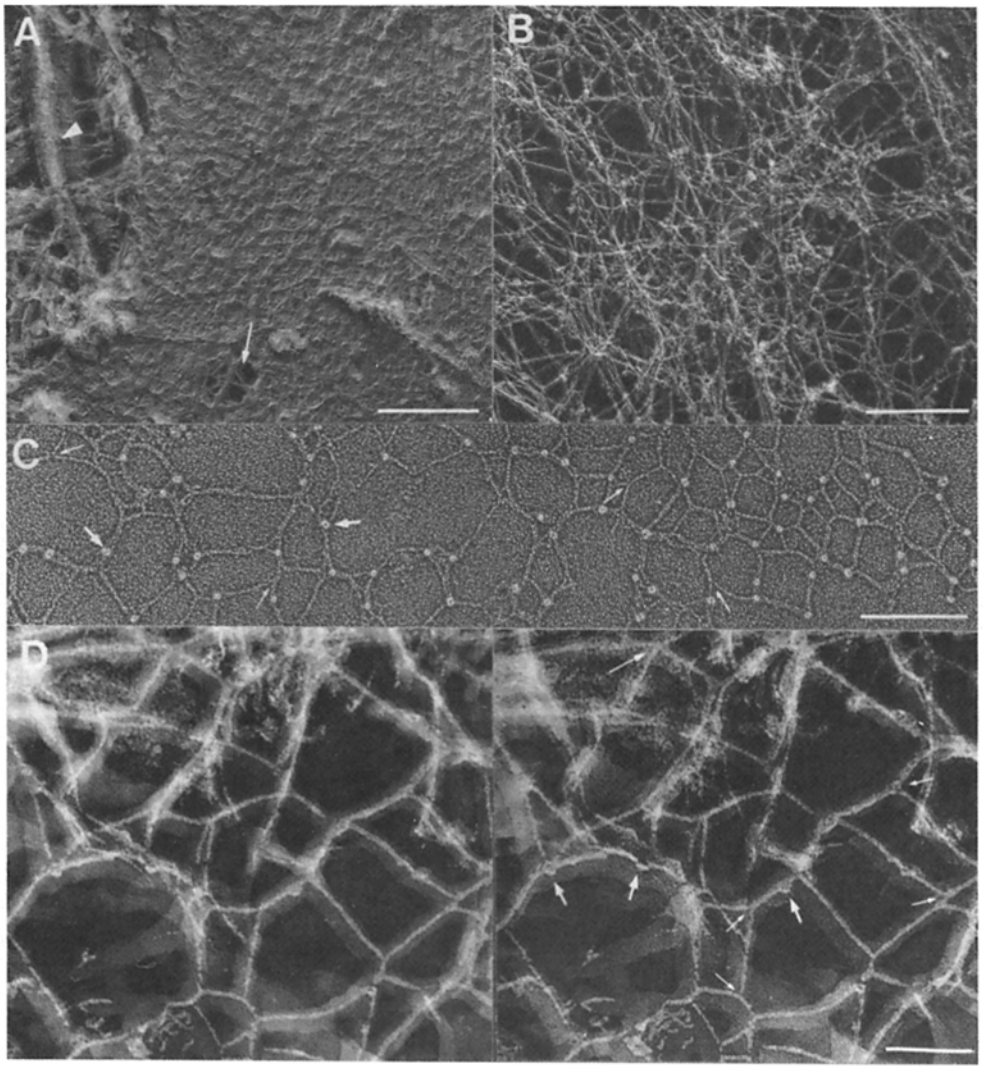

Figure 1. Pt/C replicas of amniotic basement membrane and polymerized type IV collagen. (*A*) *En face* view of amniotic membrane surface after removal of epithelial cell layer. Arrow indicates exposed region of fine branching filaments. On left side is a hole revealing underlying stroma. Example of interstitial fiber identified with arrowhead. (*B*) Amniotic basement membrane after salt extraction is seen as a sheet of delicate branching strands forming a network. (*C*) Purified EHS type IV collagen was incubated in neutral phosphate buffer, diluted into ammonium acetate buffer, sprayed onto mica, and rotary shadowed. Small thin arrows mark examples of fusion branch points and larger arrows indicate examples of globular domains. (*D*) Stereo, higher magnification view of a region of salt-extracted amniotic basement membrane network. Small thin arrows indicate examples of fusion branch points, larger arrows mark examples of globular domains, and longer thin arrow identifies two strands crossing over. The pale film around each Pt/C-coated filament is the carbon support sheath. Bars: (*A–C*) 250 nm; (*D*) 50 nm.

washed in PBS, transferred to 30% aqueous ethanol, and prepared for platinum replication as described below.

Freeze-drying and Pt/C Replication

The amniotic specimens, oriented and placed on one-half-inch filter paper disks, were rapidly plunged into a cup of liquid propane cooled in a Dewar flask of liquid nitrogen. Soluble type IV collagen in 0.1 M acetic acid was diluted to ~15 μg/ml, sprayed onto freshly cleaved mica disks, and then frozen as described above. Each disk was mounted on the precooled (−150°C) stage (23) of a modified freeze-etch unit (model 300; Balzers, Hudson, NH) fitted with electron beam guns, quartz crystal monitor, and cryopump. The chamber was evacuated and the tissue samples were freeze-dried at ~−80°C for several hours. Soluble collagen samples on mica, on the other hand, were generally only freeze-dried for 30–45 min. Each sample was then replicated without rotation with 1.0 nm of Pt/C at a 45° angle with a stage temperature of −178°C in a 5×10^{-8}-torr vacuum. The stage was then rotated during the application of 12–15 nm of carbon support backing. Tissue-derived replicas were treated with 80% sulfuric acid to remove adherent tissue, soluble collagen-derived replicas were separated from mica with hydrofluoric acid, transferred to water, and replica pieces were picked up onto 300-mesh copper grids.

Electron Microscopy

Replicas were examined in either a Phillips 420 at 80 kV with a 30-μm objective aperture or JEM 100CX at 80 kV with a 40-μm objective aperture (0.66 nm point to point resolution) at magnifications calibrated with a diffraction grating. Freeze-dried replicas were photographed, using a goniometer, in a tilt series at 10° angle intervals. Plates from rotary shadow replicas and freeze-dried replicas were contrast-reversed (22) by contact printing onto Kodak 7302 fine grain positive film before final printing. In contrast-reversed images the platinum metal appears light and regions without metal appear dark.

Results

Basement Membrane Surface

The amniotic basement membrane was exposed after detergent-aided removal of the overlying cell layer. As judged by light microscopy of stained frozen amnion sections over 95% of the cell layer was removed. The basement membrane was judged to be intact (with occasional small disruptions) by light immunofluorescence microscopy using rabbit anti-type IV collagen antibody. The Pt/C replicated surface image is that of a relatively flat and dense textured matrix (Fig. 1 *A*). Scattered on the surface are occasional holes penetrating to the underlying stroma and many small regions in which one can identify portions of a fine branching strands

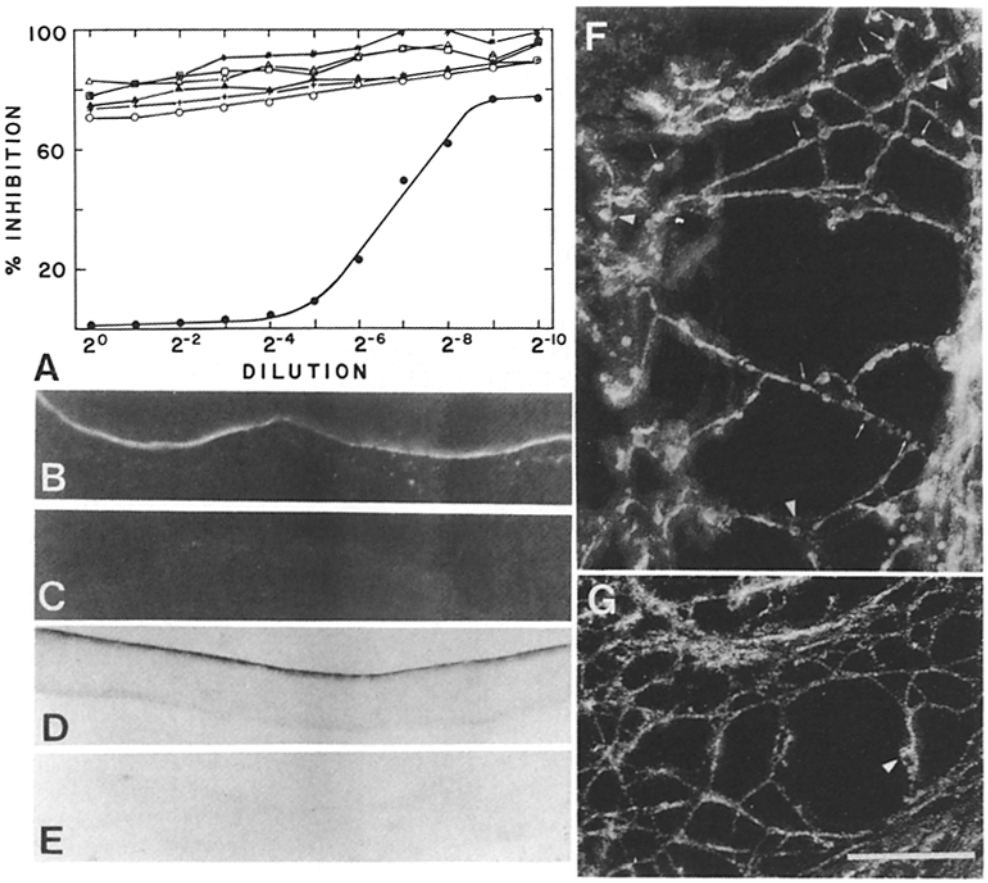

Figure 2. Type IV collagen antibody characterization and network decoration. (*A*) Competition ELISA assay in which wells were each coated with 1 μg of type IV collagen. Soluble proteins were evaluated for inhibition in twofold serial dilutions, starting at 11 μg/ml. (*Solid circles*) EHS type IV collagen; (*asterisks*) EHS low density heparan sulfate proteoglycan; (*open triangles*) EHS nidogen, 150 kD; (*open squares*) EHS laminin; (*solid triangles*) placental type V collagen; (*open circles*) placental types I and III collagen; (*crosses*) BSA. (*B* and *C*) Immunofluorescence pattern for frozen sections of human amnion incubated with either anti-type IV collagen (*B*) or preimmune rabbit IgG (*C*) followed by fluorescein-conjugated sheep anti-rabbit IgG. (*D* and *E*) Silver-enhanced pattern of 5-nm gold-tagged anti-type IV collagen (*D*) and preimmune IgG (*E*) incubated with cell-stripped salt-extracted human amnion frozen sections. (*F* and *G*) Electron micrograph of Pt/C replica of salt-extracted amniotic basement membrane network decorated with 5-nm gold-conjugated anti-type IV collagen (*F*) and 5-nm gold-conjugated preimmune IgG control (*G*) Gold particles (*small thin arrows*) conjugated to specific antibody are seen in association with the network of fine filaments. Small arrowheads mark examples of less frequent larger globular domains. Bar, 100 nm.

(Fig. 1 *A*, arrow). In the larger holes one can identify interstitial collagen fibers, ~15–40 nm in diameter (Fig. 1 *A*, left). Treatment of the amnion with a series of dissociative salt solutions, which in the EHS tumor are routinely used to extract noncollagenous components, appears to remove much of the dense matrix, leaving behind an extensive branching polygonal network of strands (Fig. 1 *B*). This extensive sheet is not seen on the stromal side (data not shown). We are reasonably confident that salt treatment and fixation have not induced substantial rearrangements of the basic network structure. First, although only small regions of network can be seen without extraction, these regions appeared to be similar to the network seen after extraction. Second, similar regions of branching network can be seen in the absence of fixation. Third, examination of plasmin-treated amnion (10 μg/ml, 37°, 2 h) exposes the same network.

Examination of the network in situ at higher magnification and in three dimensions reveals further structural detail (Fig. 1 *D*, stereopair). The network is seen as a volume-filling array of strands forming a complex irregular lattice in which the strands frequently ascend or descend from one plane to the next. These strands, forming the "sides" of the irregular polygons, are of variable but narrow metal-coated diameter ranging from 2.5 to ~7 nm; between a pair of polygonal vertices the diameter is found to be relatively constant. We interpret this to reflect variable numbers of triple-helical chains laterally associated to each other to form thicker strands. At the polygonal vertices the strands join to form "branch points," most often with three radiating arms (small thin arrows). One can also identify branch points with four radiating arms; while some of these may be produced by the contacting intersection of two straight strands (Fig. 1 *D*, small longer arrow), others, whose arms are of different diameters, are interpreted to be formed by lateral associations. Sometimes more complex branches are also identified. Structures that strictly meet morphological criteria for "naked" NH_2-terminal tetrameric domains (i.e., a thickened 30-nm-long chord with "Y" branches at each end) are rarely seen. The NH_2-terminal domains might be contained in some of the branching structures that have greater complexity (e.g., a five-arm branching structure, Fig. 4 *A*) or the four arms as pairs might even run parallel to each other.

In examining the network one can identify a carbon support sheath that surrounds each free-standing strand (e.g., Fig. 1 *D*): it is darker (less electron dense) than the platinum replica, and, because it was applied in a rotary fashion, often identifies the location of network at deeper levels even when platinum has failed to coat the filaments.

When purified type IV collagen, isolated from lathyritic EHS tumor and polymerized in vitro, is examined in low angle Pt/C rotary-shadowed replicas (Fig. 1 *C*), it is seen as an irregular (two-dimensional) polygonal network in which

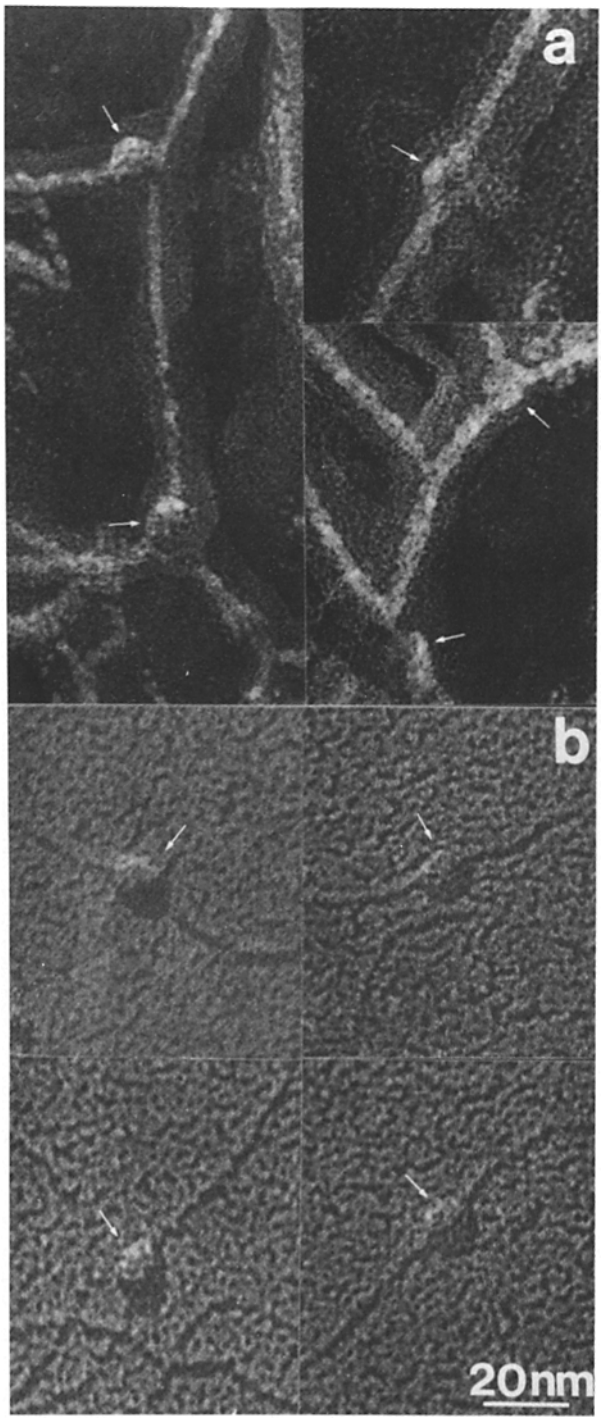

Figure 3. Comparison between globular domains of network with COOH-terminal globular domains of purified type IV collagen dimers in unidirectional Pt/C replicas. (*a*) Selected globular domains from guanidine-treated amniotic basement membrane networks. (*b*) COOH-terminal globular domains of purified EHS type IV collagen dimers sprayed in acetic acid onto mica. Arrows identify globular domains.

lateral associations are prominent contributors to the visualized structure, and is similar to the network observed in situ with strand branching (Fig. 1 *C*, small thin arrows), variable polygonal side thickness, and globular domains (larger arrows) often located at or near the branch points. While the in situ and in vitro networks possess the same basic structural features, the network formed in vitro appears about twofold less tightly meshed. A measurement of 300 in situ polygonal vertex to vertex contour distances yielded an average of 45 ± 33 nm (SD) while a measurement of 174 in vitro distances yielded an average of 109 ± 51 nm.

Antibody Characterization and Decoration of the Basement Membrane Network

Affinity-purified polyclonal rabbit anti-mouse type IV collagen antibody was evaluated for specificity of binding by competition ELISA assay with purified extracellular matrix components (Fig. 2 *A*) and by light immunomicroscopy (Fig. 2, *b–c*). Purified mouse laminin, low density heparan sulfate proteoglycan, and nidogen as well as human placental collagen types I, III, and V did not bind antibody (Fig. 2 *A*). The antibody was seen to bind both human amniotic basement membrane (Fig. 2 *B*; immunofluorescence) as well as bind the basement membranes of the glomerulus, tubules, and vessels of human and mouse kidney (not shown). Antibody coupled to 5-nm colloidal gold labeled the amniotic basement membrane. This can be seen in sections of cell-stripped, salt-extracted membranes by light microscopy (Fig. 2 *D*). Both immunofluorescence and gold-conjugated antibody staining revealed the cell-stripped basement membrane to be almost entirely intact.

When gold-conjugated antibody was incubated with amniotic basement membranes and examined as freeze-dried platinum replicas *en face* in the electron microscope (Fig. 2 *F*), the gold was seen to decorate the fine network of branching strands (small arrows indicate examples of gold particles). Background was seen to be uniformly low (Fig. 2 *G*). Accumulations of gold did not decorate the larger fibers but did decorate fine network strands that course over these fibers (not shown). These gold particles range in diameter from ~4–8 nm, consistent with the size distribution analysis provided by Janssen Pharmaceuticals for the colloidal gold (plus 1 nm of deposited Pt/C). The less frequent globular domains, integral to the network (Fig. 2, *f* and *g*, small arrowheads; see Fig. 3 for higher resolution images) were noted to be larger (10–12 nm) and could be distinguished from the gold.

Structural Elements of the Type IV collagen Network

COOH-Terminal Globular Domains. Globular structures seen in the network (Fig. 3 *a*) had essentially the same shape (slightly spheroid) and size (long axis 12 ± 2 nm; short axis 10 ± 1 nm; $n = 22$ metal-coated dimensions) as the dimeric COOH-terminal globules (Fig. 3 *b*) of freeze-dried purified type IV collagen (long axis 12 ± 1 nm; short axis 10 ± 1 nm; $n = 30$ metal-coated dimensions). The net dimensions are considered to be 9–11 nm after subtraction of the metal coat contribution (see below). We interpret the structural similarity as a morphological identification of the COOH-terminal domain of the network in situ. Compared with the globular domains replicated unidirectionally at high angle, the globules seen after low angle rotary shadow (Fig. 1 *C*) were more contrasted and exaggerated in size (14–15 nm) and therefore appear superficially more prominent.

An initial quantitative characterization of the in situ and

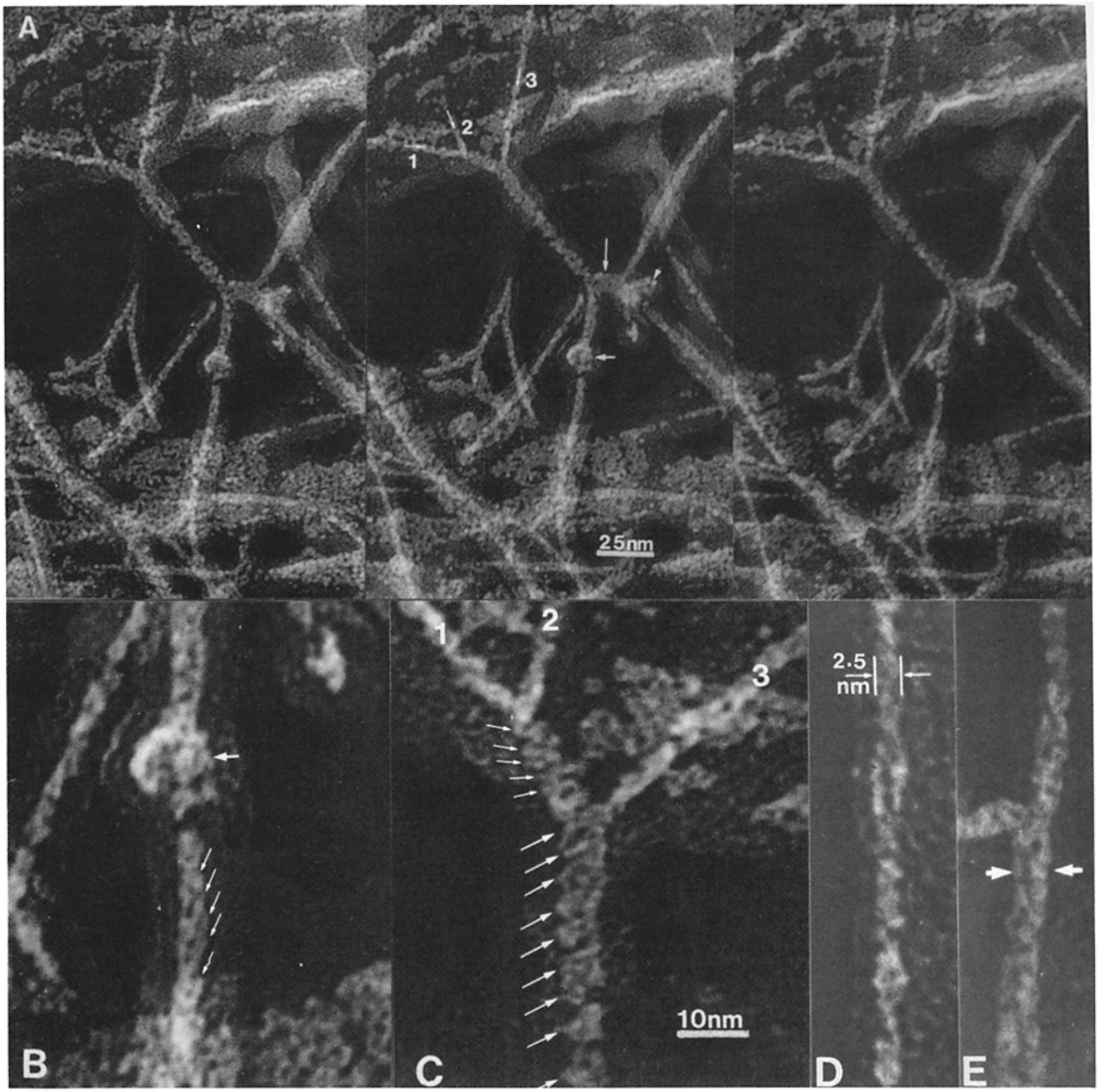

Figure 4. Macromolecular architecture of network branch points and strands. (*A*) Three-frame stereo view (each frame 10° apart) of a portion of the type IV collagen network. Three narrow filaments (2.6-nm unit filaments, see text) labeled 1–3, join to form a thicker laterally associated triple filament (~6-nm diameter). When viewed in stereo, filament 2 appears to pass under 1 and twist around it. Filament 3 then passes over 1 and 2 and twists around them. Below the second Y branch the filaments continue to twist around each other for a series of turns. In addition, a helically wrapped strand derived from two unit filaments is seen below the globular domain (*small horizontal arrow*). Small vertical arrow indicates five-arm branch point and small arrowhead marks free filament. (*B*) Detail of double filament that appears to twist around itself along strand axis. Oblique arrows mark imperfect helical crossover periodicity and horizontal arrow identifies globular domain. (*C*) Detail of region where three filaments join and appear to helically twist. (*D*) Unit filament, or thinnest filament (2.6-nm average metal-coated diameter) that is seen to fuse with other filaments to form thicker strands. (*E*) Detailed view of two unit filaments that join (just above pair of arrows) to form thicker double filament. Filament to left appears to join vertical filament from behind and then crossover ~15 nm below junction.

in vitro networks was performed. Globular domains were not regularly spaced in situ or in vitro. They could be identified along the strands of both networks with similar overall frequency. In a replicated amniotic network 4.4 globular domains were detected per micrometer of summed strand length (59 globules were counted along 13.5 μm of measured strands), whereas in a representative region of low angle-shadowed in vitro network (Fig. 1 *C*), 3.9 globular domains were identified per micrometer strand length (74 globules along 19.0 μm of strands). In comparison, one

would expect 1.2 globules per micrometer in a network held together only by end-domain interactions. The globules were often located at or near the vertices of the network; in the same amniotic network 83% (n = 59) of globular domains were noted to be within one-half diameter from a branch point compared with 81% (n = 74) in the purified type IV collagen network. In contrast, while only 20% (n = 246) of amniotic network branch points were occupied by globular domains, 50% (n = 120) of the purified type IV collagen polymer branch points were similarly occupied. These measurements suggest that the increased mesh tightness of the in situ network is due to more frequent strand branching as well as to higher two- (and presumably three-) dimensional density of COOH-terminal domains.

Lateral Associations. In many regions (Figs. 1 *D*, small short arrows, and 4, *A* and *C*), because the Pt/C-coated network is sufficiently continuous and the orientation correct, one can trace the joining of filaments to form lateral associations with a resulting increase in overall diameter distal to the fusion vertex. In Fig. 4 *A*, shown in stereo (+10°, 0°, −10°), three filaments join laterally to form a 6-nm strand. These filaments (marked 1–3) are examples of the narrowest filaments seen to laterally bind to form thicker strands and are referred to here as "unit filaments." A detailed view of a unit filament is shown in Fig. 4 *D*: it has essentially the same metal-coated thickness (2.6 ± 0.3 nm; n = 99) as the triple helical strands of purified dimers (2.8 ± 0.5 nm; n = 51) replicated in the same manner after spraying of the collagen onto mica (portions adjacent to globular domains shown in Fig. 3, bottom). The net unit filament diameter is calculated (1.7 ± 3 nm) by subtracting the thickness of the metal coat (1.0 nm minus a previously determined [24] correction factor of 0.15 nm) from the measured thickness of metal-coated filaments oriented in the same direction at the Pt/C beam, a value in agreement with the 1.5 nm expected for a triple helix. For these two reasons we conclude that the unit filament is a monomolecular filament. In Fig. 4 *E* we can trace two unit filaments that laterally join to form a thicker double filament.

Supramolecular filament twisting along the strand axis appeared to be present in many regions of the network when examined at very high magnification (Fig. 4, *A–C*). In Fig. 4, *A–C*, individual unit filaments are seen to twist around each other upon lateral association to produce double filament–twisted (Fig. 4 B) and triple filament–twisted (Fig. 4 *C*) structures. In the regions shown (and elsewhere) there is an imperfect crossover periodicity of ~5 nm. In the figure shown the filaments appear to twist in a right-handed manner; however, this must be considered a relative handedness since the absolute specimen (and thus handedness) orientation may have been lost during specimen processing. While many regions had obvious helixlike regions, many other regions were only suggestive of these patterns; sometimes laterally associated strands (Fig. 4 *E*) had a long twist crossover pattern. It is our overall impression, however, that strand twisting is widespread and a characteristic of lateral assembly.

Model

A three-dimensional wire and bead model of the network was constructed, photographed, and traced in stereo (Fig. 5). This model reflects essential binding structural features and should be regarded as an approximation of the structural complexity present in the amnion.

Discussion

In this study we have analyzed, in situ, molecular architectural features of the amniotic basement membrane collagen network using a high resolution metal shadow casting technique coupled with selective extraction, decoration with gold-conjugated polyclonal antibody, and morphometry. This network is a layered polygonal mesh of laterally (side by side) associated branching monomolecular filaments. Supramolecular filament twisting can be detected, and globular structures, which we interpret as the COOH-terminal dimeric domains, are integral to this network.

Basement Membrane Collagen Network In Situ and In Vitro

The structure visualized in situ supports essential features of the lateral and end-domain association model derived from in vitro data and proposed earlier (29, 31). Both in situ and in vitro networks have extensive lateral associations of single molecular filaments and are seen to frequently branch to form an array with sides from one to several triple helical filaments thick. In both networks the globular domains, sites of COOH-terminal linear dimerization, are often noted to be located at or near the polygonal vertices. While structures identical to the isolated NH_2-terminal tetrameric region are only infrequently observed, we suspect that in most cases this domain is present with greater structural complexity produced by superimposed lateral associations. Using domain-specific antibody, it should be possible to better characterize the in situ architectural relationships of this unique structure.

On the other hand, the appearance of the network in the amnion is not compatible with a model (26) in which type IV collagen monomers are connected only at their amino tetrameric and carboxyl globular domains. With such a network one would expect to find that the branch point to branch point (here NH_2-terminal to NH_2-terminal tetrameric domain) contour distance would be ~800 nm (26), the only Y branches seen would be 30-nm-spaced pairs (7S) and all filaments would be of the same diameter equal to the unit filament.

The similarity between the network identified in the amnion with that formed in vitro indicates that type IV collagen dimers, when incubated in neutral phosphate buffer, can recapitulate by mass action, to a first approximation, the assembled architecture they normally assume in a basement membrane and that the basic assembly information is encoded in the dimers. It can be argued that a structurally correct or nearly correct basement membrane scaffolding can be formed simply by cell secretion of type IV collagen to an appropriate concentration into a diffusion-limiting compartment; this compartment would be bounded on one side by an absolute barrier, the cell plasma membrane, and on the other by a relative diffusion barrier, the stroma.

While the in situ and in vitro networks are quite similar, some differences can be appreciated between them. The principal difference (apart from the latter seen in two dimensions and the former in three dimensions) is that the former,

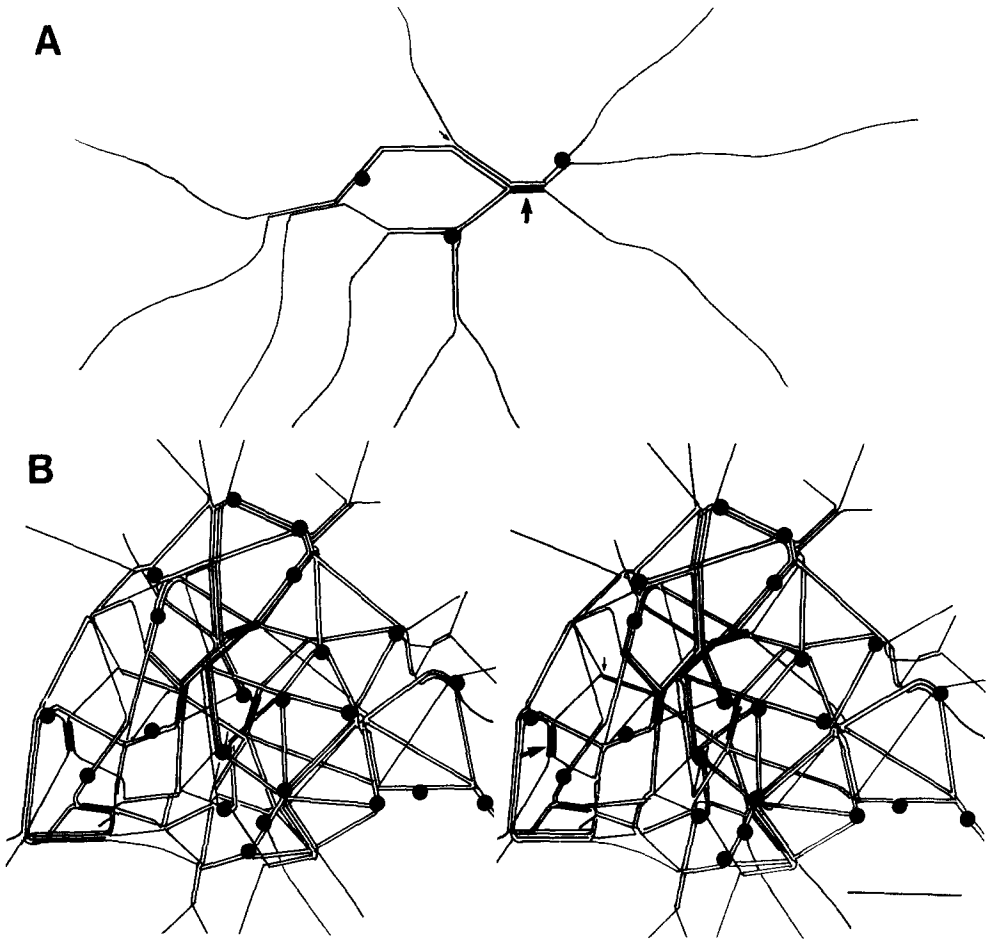

Figure 5. Schematic model for the macromolecular architecture of polymerized type IV collagen. Network structure is dependent upon lateral associations with branching of filaments as well as NH_2-terminal tetrameric acid and COOH-terminal dimeric domains. (*A*) Simplified scheme of the three different types of binding interactions. Larger arrow indicates NH_2-terminal tetrameric domain, here shown with a laterally associated filament; smaller arrow indicates branch point with distal lateral association of triple helical strands. Solid circles represent COOH-terminal globular domains. (*B*) Stereopair drawn from photographs of a three-dimensional wire and bead model revealing three-dimensional irregular polygonal network of greater complexity reflecting molecular architecture found in situ. Bar, 100 nm.

in most (although not all) fields examined, has a tighter mesh than the latter. In this study most amniotic intervertex distances appear to be closer to ~45 nm, while those of a reconstituted polymer are closer to 100 nm. At present we can only speculate on the reason for these spacing differences. An analogy can be made with the interstitial collagens where heterogeneity of subfibril spacing, reflected in banding pattern, has been observed in reconstituted fibers (4, 5), perhaps produced by alterations of self-assembly environmental conditions. Similarly, in type IV collagen, network spacing may be dependent on pH, salts, protein concentration or, in the case in situ, the modulating action of other matrix macromolecules or even the cell surface. In examining the network of the amnion we have on occasion found regions to be considerably more open with increased vertex to vertex spacing. While representing a preliminary finding, this observation raises the possibility that regional mesh size heterogeneity exists in vivo and that there might be specific mechanisms by which a cell can regulate mesh tightness.

Network Geometry In Situ

The three-dimensional structure of the network in situ is complex and the irregularity of polygonal dimensions indicates that each dimer has more than a single allowed spatial relationship with a neighboring dimer. The binding rules that determine these relationships are not yet known; we speculate that the branch point locations may be determined by some of the irregularly spaced interruptions of the gly-x-y repeat sequence (28) related to sites of flexibility (11) along the collagen chain. Previously (29, 31) we suggested that type IV collagen might form a crystalline-like lattice using lateral and end-domain interactions. The study reported here does not substantiate this since the interglobular and intervertex distances are not uniform.

More regular order exists at the level of the laterally associated filament. First filament thickness is found to lie in a fairly narrow range, reflecting a relatively stringent limitation in the number of unit molecular filaments that can laterally associate. Second, we have evidence for double and higher order unit filament twisting. We are curious as to whether there might be a relationship between a 10-nm repeat along the filament axis reported in a recent x-ray diffraction study of stretched lens capsule (2) and the helixlike strands detected in the amnion (realizing the actual strand twist periodicity might have been altered by stretching). Of the other collagens, type VI has also been found to possess a superhelicity in its double-stranded rodlike regions (9).

Network Assembly

The proposal that supramolecular filament twisting along the strand axis is an inherent property of lateral assembly has important consequences for overall network structure and assembly. First, lateral associations in which supramolecular helices form, even if produced by relatively weak noncova-

lent interactions, would lead to a stable structure once the amino and carboxyl end-domains were "locked" into the network to form what can be regarded as intertwined "closed loops": the laterally associated monomolecular filaments could not be undone unless the covalently bound chains or the ends of the collagen were broken apart. Second, where this twisting is present, lateral assembly would have occurred with one or more free collagen ends that must rotate around each other to form the supramolecular helices before closure of the loops. This bears on the question of bonding sequence in network formation (3, 6, 17, 29). Examination of the self-assembly of collagen dimers derived from EHS tumor (29) led to the proposal that COOH-terminal dimer formation occurs first, lateral association second, and NH_2-terminal tetramer formation last, while studies on tissue culture–derived collagen monomers (6, 17) and collagen extracts from developing tissue (3) led to the proposal that tetramer formation is an initial event in network formation. These apparent discrepancies might be resolved by the consideration (3) that assembly of the network could proceed by several parallel paths in which steps of assembly (before covalent cross-linking) are path independent. In those regions where NH_2- and COOH-terminal bonds have first formed closed loops we would expect to find an absence of supramolecular filament twisting.

Universality of Model

Electron microscopic studies of a variety of basement membranes have revealed architectural heterogeneity with respect to thickness, number of layers, and the presence, in some, of geometric structure. Furthermore, biochemical studies have revealed differences in the relative amounts of basement membrane components (reviewed in reference 31). While we do not know if all basement membrane collagen networks display the same basic architectural features seen in this study, we predict that the network of the amnion will prove to be typical of many basement membranes. First, the basement membrane studied has a cross-sectional morphology that can be regarded as representative of many simple basement membranes. Second, the same network is seen in the mouse EHS tumor matrix (Yurchenco, P. D., and G. C. Ruben, manuscript in preparation). Third, the overall pattern of the plasmin-exposed network of Reichert's membrane (12) as well as the fine irregular (as opposed to the larger hexagonal) network seen in Descemet's membrane (25) are suggestively similar when examined in retrospect. Fourth, there is x-ray diffraction evidence of lateral association of triple helical filaments to form strands in the basement membrane network of lens capsule (2). Fifth, basement membranes contain the same basic type IV collagen molecular "building block." If there is heterogeneity of the basement membrane molecular architecture, it may instead be found in the other components. Using the replication technique described in this study along with differential extraction and domain-specific antibody decoration it should be possible to study the structural relationships of these other components to address this and other questions.

We would like to thank Yi-Shan Cheng, Caroline Wong, and Kurt Barkalow for their expert technical assistance; David Birk for his helpful suggestions for developing the antibody binding conditions; and Robert L. Trelstad for his critical advice.

This study was supported by Public Health Service grant R01-DK36425 (P. D. Yurchenco) and by a Sinsheimer Scholarship Award (P. D. Yurchenco). P. D. Yurchenco is a Hartford Foundation Fellow. G. C. Ruben was supported by GeoM Co. and thanks the Ripple EM Laboratory at Dartmouth.

Received for publication 27 March 1987, and in revised form 7 August 1987.

References

1. Bachinger, H. P., L. I. Fessler, and J. H. Fessler. 1982. Mouse procollagen IV characterization and supramolecular assembly. *J. Biol. Chem.* 257:9796–9803.
2. Barnard, K., L. J. Gathercole, and A. J. Bailey. 1987. Basement membrane collagen: evidence for a novel molecular packing. *FEBS (Fed. Eur. Biochem. Soc.) Lett.* 212:49–52.
3. Blumberg, B., L. I. Fessler, M. Kurkinen, and J. H. Fessler. 1986. Biosynthesis and supramolecular assembly of procollagen IV in neonatal lung. *J. Cell Biol.* 103:1711–1719.
4. Bruns, R. R., R. L. Trelstad, and J. Gross. 1973. Cartilage collagen: a staggered substructure in reconstituted fibrils. *Science (Wash. DC).* 181: 269–271.
5. Bruns, R. R. 1976. Supramolecular structure of polymorphic collagen fibrils. *J. Cell Biol.* 68:521–538.
6. Duncan, K. G., L. I. Fessler, H. P. Bachinger, and J. H. Fessler. 1983. Procollagen IV: associations to tetramers. *J. Biol. Chem.* 258:5869–5877.
7. Farquhar, M. G. 1982. Structure and function in glomerular capillaries: role of the basement membrane in glomerular filtration. *In Biology and Chemistry of Basement Membranes.* N. A. Kefalides, editor. Academic Press, Inc., New York. 43–80.
8. Fessler, L. I., and J. H. Fessler. 1982. Identification of the carboxyl peptides of mouse procollagen IV and its implications for the assembly and structure of basement membrane procollagen. *J. Biol. Chem.* 257:9804–9810.
9. Furthmayr, H., H. Wiedemann, R. Timpl, E. Odermatt, and J. Engel. 1983. Electron microscopical approach to a structural model of intima collagen. *Biochem J.* 211:303–311.
10. Hassel, J. R., W. C. Leyshon, S. R. Ledbetter, B. Tyree, S. Suzuki, M. Kato, K. Kimata, and H. K. Kleinman. 1985. Isolation of two forms of basement membrane proteoglycans. *J. Biol. Chem.* 260:8098–8105.
11. Hofmann, H., T. Voss, K. Kuhn, and J. Engel. 1984. Localization of flexible sites in thread-like molecules from electron micrographs: comparison of interstitial, basement membrane and intima collagens. *J. Mol. Biol.* 172:325–343.
12. Inoue, S., C. P. Leblond, and G. W. Laurie. 1983. Ultrastructure of Reichert's membrane, a multilayered basement membrane in the parietal wall of the rat yolk sac. *J. Cell Biol.* 97:1524–1537.
13. Liotta, L. A., C. W. Lee, and D. J. Marakis. 1980. New method for preparing large surfaces of intact human basement membrane for tumor invasion studies. *Cancer Lett.* 11:141–152.
14. Madri, J. The preparation of type V (AB_2) collagen. *In* Immunochemistry of the Extracellular Matrix. Vol. I. H. Furthmayr, editor. CRC Press, Inc., Boca Raton, FL. 75–89.
15. Madri, J. A., and S. K. Williams. 1983. Capillary endothelial cell cultures: phenotypic modulation by matrix components. *J. Cell Biol.* 97:153–165.
16. Modesti, A., T. Kalebic, S. Scarpa, S. Togo, G. Grotendorst, L. A. Liotta, and T. J. Triche. 1984. Type V collagen in human amnion is a 12 nm fibrillar component of the pericellular interstitium. *Eur. J. Cell Biol.* 35:246–255.
17. Oberbaumer, I., H. Wiedemann, R. Timpl, and K. Kuhn. 1982. Shape and assembly of type IV procollagen from cell culture. *EMBO (Eur. Mol. Biol. Organ.) J.* 1:805–810.
18. Paulsson, M., M. Aumailley, R. Deutzmann, R. Timpl, K. Beck, and J. Engel. 1987. Laminin-nidogen complex: extraction with chelating agents and structural characterization. *Eur. J. Biochem.* 166:11–19.
19. Risteli, J., H. P. Bachinger, J. Engel, H. Furthmayr, and R. Timpl. 1980. 7-S collagen: characterization of an unusual basement membrane structure. *Eur. J. Biochem.* 108:239–250.
20. Roll, F. J., J.A. Madri, J. Albert, and H. Furthmayr. 1980. Codistribution of collagen types IV and AB_2 in basement membranes and mesangium of the kidney: an immunoferritin study of ultrathin frozen section. *J. Cell Biol.* 85:597–613.
21. Ruben, G. C., and K. A. Marx. 1984. Real fibre diameters from freeze-etched Pt-C replicated fibre images: a DNA study. *Proc. Annu. Meet. Electron Microsc. Soc. Am.*, 42nd, Detroit. 684–685
22. Ruben, G. C., and K. A. Marx. 1984. Parallax measurements on stereomicrogaphs of hydrated single molecules: their accuracy and precision at high magnification. *J. Electron Microsc. Tech.* 1:373–385.
23. Ruben, G. C. 1985. A comparison of specimen stage surface temperature and the GA1 control unit reading in Balzers freeze microtome cold stage. *J. Electron Microsc. Tech.* 2:53–57.
24. Ruben, G. C., and G. H. Bokelman. 1987. Triple stranded, left hand

twisted cellulose microfibril. *Carbohyd. Res.* 160:434–443.
25. Sawada, H. 1982. The fine structure of the bovine Descemet's membrane with special reference to biochemical nature. *Cell & Tissue Res.* 226:241–255.
26. Timpl, R., H. Wiedemann, V. Van Delden, H. Furthmayr, and K. Kuhn. 1981. A network model for the organization of type IV collagen molecules in basement membranes. *Eur. J. Biochem.* 120:203–211.
27. Tsilibary, E. C., and A. S. Charonis. 1986. The role of the main noncollagenous domain (NC1) in type IV collagen self-assembly. *J. Cell Biol.* 103:2467–2473.
28. Schwartz, U., D. Schuppan, I. Oberbaumer, R. W. Glanville, R. Deutzmann, R. Timpl, and K. Kuhn. 1986. Structure of mouse type IV collagen: amino acid sequence of the C-terminal 511-residue-long triple-helical segment of the α2(IV) chain and its comparison with the α1(IV) chain. *Eur. J. Biochem.* 157:49–56.
29. Yurchenco, P. D., and H. Furthmayr. 1984. Self-assembly of basement membrane collagen. *Biochemistry.* 23:1839–1850.
30. Yurchenco, P. D., Y. S. Cheng, and G. C. Ruben. 1987. Self assembly of a high molecular weight basement membrane heparan sulfate proteoglycan into dimers and oligomers. *J. Biol. Chem.* In press.
31. Yurchenco, P. D., E. C. Tsilibary, A. S. Charonis, and H. Furthmayr. 1986. Models for the self-assembly of basement membrane. *J. Histochem. Cytochem.* 34:93–102.